Vol.65: e22210281, 2022
https://doi.org/10.1590/1678-4324-2022210281
ISSN 1678-4324 Online Edition

Article - Human and Animal Health

Comparative Study of High-throughput Screening Models for Anti-hyperpigmentation Compounds

Tingwei Sun[1]
https://orcid.org/0000-0001-6832-4931

Qingquan Guo[1]
https://orcid.org/0000-0002-2232-057X

Shaojuan Wu[1]
https://orcid.org/0000-0001-9328-3043

Kui Su[2]
https://orcid.org/0000-0002-6304-9907

Jingwen Lun[2]
https://orcid.org/0000-0003-4149-4193

Yihan Zhang[2]
https://orcid.org/0000-0002-4815-9657

Wen Tan[2]
https://orcid.org/0000-0001-7092-8910

Haishan Zhao[3*]
https://orcid.org/0000-0001-7355-4627

[1]Guangdong University of Technology, School of Chemical Engineering and Light Industry, Guangzhou, Guangdong, China; [2]Guangdong University of Technology, School of Biomedicine and Pharmaceutical Sciences, Guangzhou, Guangdong, China; [3]Guangdong Provincial Key Laboratory of South China Structural Heart Disease, Guangdong Cardiovascular Institute, Guangdong Provincial People's Hospital, Guangdong Academy of Medical Sciences, Guangzhou, China.

Editor-in-Chief: Alexandre Rasi Aoki
Associate Editor: Najeh Maissar Khalil

Received: 18-May-2021; Accepted: 02-May-2022

*Correspondence: hartzhao@163.com; (H.Z.).

HIGHLIGHTS

- It is the first time to compare mushroom tyrosinase model, B16 mouse melanoma cell model and zebrafish model.
- A high-throughput method for the quantification of melanin in zebrafish skin based on the Phyton for the first time.

Abstract: The mushroom tyrosinase assay, B16-F10 mouse melanoma cell model, and zebrafish model are frequently used for high-throughput screening and are widely used for developing anti-hyperpigmentation compounds, although these systems cannot be compared. We used each of these three systems to evaluate the seven anti-hyperpigmentation compounds. We investigated 1. tyrosinase activity using a mushroom tyrosinase assay, 2. viability, tyrosinase activity, and melanin content in B16-F10 cells, and 3. embryonic toxicity, tyrosinase activity, and melanin content in zebrafish. α-Arbutin, raspberry ketone (RK), raspberry ketone glucoside (RKG), glabridin (GLA), and 3-o-ethyl-ascorbic (EA), inhibited the activity of mushroom tyrosinase; dipotassium glycyrrhizinate (DG) did not inhibit mushroom tyrosinase activity, and glycyrrhetic acid (GA) promoted tyrosinase activity. Tyrosinase activity was inhibited by α-arbutin, GLA, GA and DG in B16-F10 cells; RK, RKG and EA did not inhibit tyrosinase activity. α-Arbutin, RK, RKG, EA, and GA, inhibited tyrosinase activity in zebrafish; GLA and DG did not inhibit tyrosinase activity. α-arbutin, RK, RKG, EA, GLA, and DG reduced melanin synthesis in B16-F10 cells in a dose-dependent manner without significant toxicity; GA did not inhibit melanin synthesis. α-arbutin, RK, RKG and GA significantly reduced melanin content on the zebrafish body surface. Mushroom tyrosinase analysis was the most practical assay among the three

systems but had poor reliability. The B16-F10 mouse melanoma cell system was the most sensitive but had the worst stability. The zebrafish system had better reproducibility than other systems; however, most compounds were difficult to screen in this system.

Keywords: Melanin; Zebrafish; B16-F10 mouse melanoma cell; Whitening ingredient.

INTRODUCTION

Melanin is produced from melanocytes in the epidermis, which can absorb ultraviolet (UV) radiation from the sun and protect the skin from the damaging effects of reactive oxygen species and free radicals [1]. However, abnormal accumulation of pigmentation causes hyperpigmentation and skin diseases. These include chloasma, freckles, age spots, melasma, and melanoma [2]. It is necessary to develop more effective and safer anti-hyperpigmentation compounds to inhibit excessive skin pigmentation. Increasing research requires a high-throughput and economic whitening efficacy evaluation model [3]. The three most frequently used models for high-throughput screening are the mushroom tyrosinase assay (MTA), B16-F10 mouse melanoma cell model, and zebrafish model.

Tyrosinase levels are an important part of the melanin synthesis process, as decreased tyrosinase production correlates with reduced melanin pigmentation, which leads to skin whitening [4]. Tyrosinase catalyzes the hydroxylation of L-tyrosine to L-DOPA in addition to the oxidation of o-diphenol to the corresponding quinone. L-dopaquinone is the rate-limiting enzyme in melanin synthesis [5]. L-DOPA was used as a substrate to test whether anti-hyperpigmentation compounds could inhibit tyrosinase activity[6]. MTA has the advantages of simple operation, low experimental cost, and low threshold of experimental development. B16-F10 cells can simulate the physiological environment of the human body through cell culture. This model can be used to determine whether anti-hyperpigmentation compounds can inhibit tyrosinase activity and melanin production without individual differences. The zebrafish model is widely used for high-throughput screening [7, 8]. The effects of anti-hyperpigmentation compounds on the development of zebrafish embryos and the formation of melanin on the zebrafish surface can be observed directly under a stereomicroscope [7].

These three models are widely used in developing anti-hyperpigmentation compounds, but there has been no comparison among them. Paradoxical results have been reported for these methods. For example, GLA can inhibit the activity of MTA and melanin production and tyrosinase activity in B16-F10 cells [9, 10]. However, GLA did not inhibit melanin production in zebrafish [10]. Thus, further investigations and comparisons are required. To compare these models, we selected a representative batch of anti-hyperpigmentation compounds from the official whitening list published by the Chinese mainland, South Korea, and Taiwan [11, 12], as shown in Figure 1.

In this study, we evaluated these compounds with MTA, B16-F10 cells, and zebrafish for high-throughput and rapid detection of anti-hyperpigmentation compounds, and explored the differences and relationships among the three models.

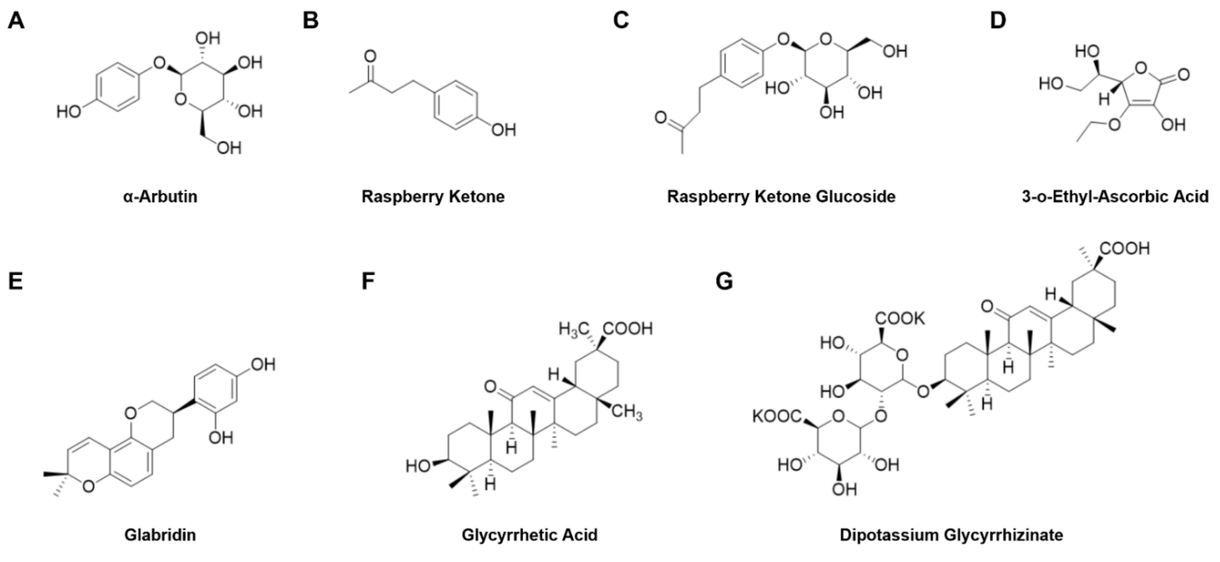

Figure 1. Structures of compounds examined in this study.

Chemicals and Compounds

L-DOPA, mushroom tyrosinase, and raspberry ketone (4-(4-Hydroxyphenyl)-2-butanone) were purchased from Aladdin (Shanghai, China). EA (3-o-Ethyl-Ascorbic) and α-arbutin (3-β-Hydroxy-11-oxoolean-12-en-30-oic acid) was purchased from Teelar Biotechnology (Guangzhou, China). Raspberry ketone glucoside (4-[4-(β-d-glucopyranosyloxy)phenyl]-2-butanone) was purchased from Yuanye (Shanghai, China). Glabridin (4-[(3R)-8,8-Dimethyl-3,4-dihydro-2H-pyrano [6,5-f]chromen-3-yl]benzene-1,3-diol) was purchased from Aoli (Shanghai, China). Dipotassium glycyrrhizinate was purchased from Bioherbix (Xian, China). All other chemicals and reagents used were of analytical grade.

Mushroom Tyrosinase Activity Assay

The assay was performed using a modified method adapted from previous studies [6]. Inhibition of tyrosinase activity was analyzed according to previous studies, with some modifications. L-DOPA solution (280 μL) (0.5 mM) was dissolved in 50 mM phosphate buffer (pH 6.8) and then added to 10 μL of the whitening ingredient dissolved along the concentration gradient. After 10 min of incubation at 37 °C, 10 μL of mushroom tyrosinase (400 U/mg, dissolved in 50 mM phosphate buffer, pH 6.8) were added to the mixture. The absorbance of the mixture at 475 nm was measured using a plate reader (TriStar2 LB942, Berthold Technologies, Bad Wildbad, Germany) against the phosphate buffer as a background value every 20s for 30 min. The slope of the correlation between the absorbance and time was calculated. The reaction mixture without the sample was used as a control. The mushroom tyrosinase activity was calculated as follows:

$$A_{mt}=\frac{S_{ae}-S_{ab}}{S_{ac}-S_{ab}}\times 100\%$$

S_{ae} = Slope of experiment absorbance value
S_{ab} = Slope of background absorbance value
S_{ac} = Slope of control absorbance value
A_{mt} = Mushroom tyrosinase activity

B16-F10 Mouse Melanoma Cells Model

Cell Culture

B16-F10 cell culture was performed according to previously reported methods, with modifications [13]. B16-F10/F10 murine melanoma cells were purchased from Zhongqiao Xinzhou Biotechnology (Shanghai, China). The cells were cultured in Roswell Park Memorial Institute (RPMI) 1640 medium (Gibco, Shanghai, China) containing 10 % fetal bovine serum (FBS) (Gibco) and 100 U/mL of penicillin/streptomycin (Gibco). The cell line was cultured in 100 mm culture dishes (Corning, Shanghai, China) at 37 °C with 5 % carbon dioxide (CO_2) in fully humidified air. B16-F10 cells were attached to the surface of the culture dish. The culture medium was changed every alternate day. B16-F10 cells were harvested by trypsinization using trypsin-EDTA (0.05 %) and phenol red (Gibco). The subcultures were prepared by trypsinization, and the sub-cultivation ratio was 1:4 (culture: medium). Cells were seeded at an appropriate seed density for four hours and then treated with various drug concentrations. Cells were harvested 48 h post-treatment (hpt).

CCK8 assay

The CCK8 assay was performed using a CCK8 kit following the manufacturer's protocol (TransGen, Beijing, China). Briefly, cells were plated into 96-well plates (1×10^3 cells per well) (Jet Biofil, Guangzhou, China) in 100 μL of culture medium, incubated for four hours, and replaced with new culture media containing different concentrations of anti-hyperpigmentation compounds. After incubation for 24 h, CCK-8 solution (10 μL/well) was added to the culture medium (100 μL/well) for two hours. The absorbance of the mixture at 450 nm was measured using a plate reader (TriStar2 LB942, Berthold Technologies, Bad Wildbad, Germany). The cell survival rates were calculated as follows:

$$C_{sr}=\frac{A_e-A_b}{A_c-A_b}\times 100\ \%$$

A_e = Absorbance of the experimental group
A_b = Absorbance of the background group
A_c = Absorbance of the control group
C_{sr} = Cell survival rate

The maximal concentration with no inhibition of cell viability was used as the optimal concentration. Each experiment was repeated thrice.

Cells Tyrosinase Activity and Melanin Content Assay

Tyrosinase activity and melanin content assays were performed according to previously reported methods with modifications [14]. B16-F10 cells were seeded into a 6-well plate (Jet Biofil, Guangzhou, China) at a density of 1 × 10^5 cells per well in DMEM and allowed to attach for 4 h. The medium was replaced with fresh DMEM containing various concentrations of each compound. The cells were cultured for 48 h. After washing with PBS, cells were detached using a scraper and placed in a 1.5 mL EP tube. Total protein extraction reagent (200 μL; BestBio, Shanghai, China) was added to extract total protein per tube, after centrifugation at 13500 *g* for 15 min at 4 °C (5424 Eppendorf, Hamburg, Germany). The resulting supernatant was used as total protein extract. Total protein extracts from cells were used in tyrosinase activity assays. Twenty microliters of the extract were used to quantify the total protein concentration using the BCA protein assay kit (BestBio).

Total protein extract (100 μL) was transferred to the wells of a 96-well plate, followed by the addition of 100 μL of 0.5 mM L-DOPA. The absorbance of the mixture at 475 nm was measured using a plate reader against the phosphate buffer as a background value per 20 s for one hour. The slope of the correlation between the absorbance and time was calculated. The tyrosinase activity was calculated as follows:

$$A_{ct}=\frac{(S_{ae}-S_{ab})/C_{ep}}{(S_{ac}-S_{ab})/C_{cp}}\times 100\%$$

S_{ae} = Slope of the experimental group absorbance value
S_{ab} = Slope of the background group absorbance value
S_{ac} = Slope of the control group absorbance value
C_{ep} = Concentration of the experimental group protein
C_{cp} = Concentration of the control group protein
A_{ct} = Cell tyrosinase activity

The precipitate in the EP tube was added to 60 μL of DMSO (MP Biomedical, Irvine, CA, USA) and homogenized in a water bath sonicator for one hour before dosing. The melanin homogenizer was then transferred to a 96-well plate. The absorbance of the mixture at 475 nm was measured using a plate reader against the total protein extraction reagent as the background value.

Cell melanin content was calculated as:

$$C_{mc}=\frac{(A_e-A_b)/P_e}{(A_c-A_b)/P_c}\times 100\%$$

A_e= Absorbance of the experimental group
A_b= Absorbance of the background group
A_c= Absorbance of the control group
P_e= Protein concentration of the experimental group
P_c= Protein concentration of the control group
C_{mc}= Cell melanin content

Zebrafish Model

Zebrafish Maintenance and Breeding

Zebrafish embryos were obtained and raised, and the fish were maintained as previously described [15]. Zebrafish wild-type AB (*Danio rerio* AB) was obtained from the China Zebrafish Resource Center (Wuhan, China), and three-month-old zebrafish were used for embryo production. Sexually mature zebrafish were maintained in a recirculating aquaculture system (Shanghai Haisheng, Shanghai, China) at 28.0 °C ± 1.0 °C. The day to night photoperiod was 14 h: 10 h. $NaHCO_3$ and NaCl were used to adjust the pH and conductivity at pH 6.8~7.4 and 500~550 μS. Mature zebrafish were fed Artemia salina (Chaoying, Tianjin, China) twice daily. Males and females were maintained separately until the night before spawning at a ratio of 2:1 or 1:1. Embryos were obtained by natural mating. Embryos were raised at 28 °C in Holtfreter's solution (60 mM NaCl, 2.4 mM $NaHO_3$, 1 mM $CaCl_2$, and 1.34 mM KCl). Embryo and larval developmental stages are expressed in hours post fertilization (hpf).

Zebrafish Safety Concentration Assay

The zebrafish safety concentration assay was performed as described previously [15]. Wild-type zebrafish embryos were cleaned and grown in 24-well plates (Jet Biofil) at 28 °C. Each well contained 1000 µL of Holtfreter's solution and 15 embryos. Three wells were used as the groups. Serial concentrations of anti-hyperpigmentation compounds of 1000 µL were added to each well at 24 hpf. Holtfreter's solution or 1 % DMSO was used as the solvent control. Zebrafish embryos were observed using a Stemi 508 stereomicroscope (Carl Zeiss, Jena, Germany). The maximal concentration was determined based on the morphological appearance and development of zebrafish embryos. Experiments were repeated at least thrice.

Zebrafish Tyrosinase Activity and Melanin Content Assay

The experimental procedure was the same as that described in Section 3.2, and the ingredient concentration was determined from the experimental results in Section 4.2. Ten embryos were placed in a 1.5 mL EP tube, and 150 µL of total protein extraction reagent was added. In addition to 100 µL total protein extract and 100 µL L-DOPA per well, the preprocessing method was identical to that described in Section 2.3. Zebrafish tyrosinase activity was calculated as follows:

$$A_{zt}=\frac{(S_{ae}-S_{ab})/P_e}{(S_{ac}-S_{ab})/P_c}\times 100\%$$

S_{ae}= Slope of the experimental group absorbance value
S_{ab}= Slope of the background group absorbance value
S_{ac}= Slope of the control group absorbance value
P_e = Protein concentration of the experimental group
P_c = Protein concentration of the control group
A_{zt} = Zebrafish tyrosinase activity

Three embryos were randomly selected from each experimental group. Embryos were immobilized on their sides on slides using 3 % methylcellulose (Yuanye). Images were visualized using a Stemi 508 stereomicroscope (Carl Zeiss) and captured using an Axio Imager A2 digitizing morphometry system (Carl Zeiss). The traditional method for melanin content quantification is labor-dependent. Therefore, we developed a Python program. Based on this program, zebrafish images were processed using the OpenCV library in Python. The initial step was to convert the RGB image into a grayscale image. The Canny edge detector is an edge detection operator that uses a multi-stage algorithm to detect a wide range of edges in images. Melanin on the zebrafish body surface was transformed into black spots, and then the number and area were counted. The rules of image background filtering were determined through a batch statistical analysis of the experimental images. After treatment, the effect of anti-hyperpigmentation compounds on the melanin content of the zebrafish body surface can be obtained directly and quickly.

Zebrafish melanin content was calculated as:

$$C_{zm}=\frac{V_e}{V_c}\times 100\%$$

V_e= Value of the experimental group
V_c= Value of the background group
C_{zm}= Zebrafish melanin content

Statistical Analysis

Statistical analysis was performed using GraphPad Prism 8 (GraphPad Software Inc., La Jolla, CA, USA), and the data are presented as the mean SEM. The results were further analyzed using Student's *t*-test, and p values less than 0.05 were considered statistically significant.

RESULTS

Mushroom Tyrosinase Assay

To compare the anti-hyperpigmentation capabilities of these compounds, we first evaluated them using MTA. As shown in Figure 2, we found that five of the seven compounds inhibited mushroom tyrosinase activity: α-arbutin, RK, RKG, GLA, and EA. The maximum inhibitory concentrations of these five compounds were α-arbutin (16.21 %, 100 mM), RK (68.77 %, 10 mM), RKG (77.21 %, 600 mM), GLA (43.55 %, 40 μM), and EA (1.48 %, 1 M). DG had no inhibitory effect on the mushroom tyrosinase activity. GA promoted tyrosinase activity by 204.18 % at 4 mM.

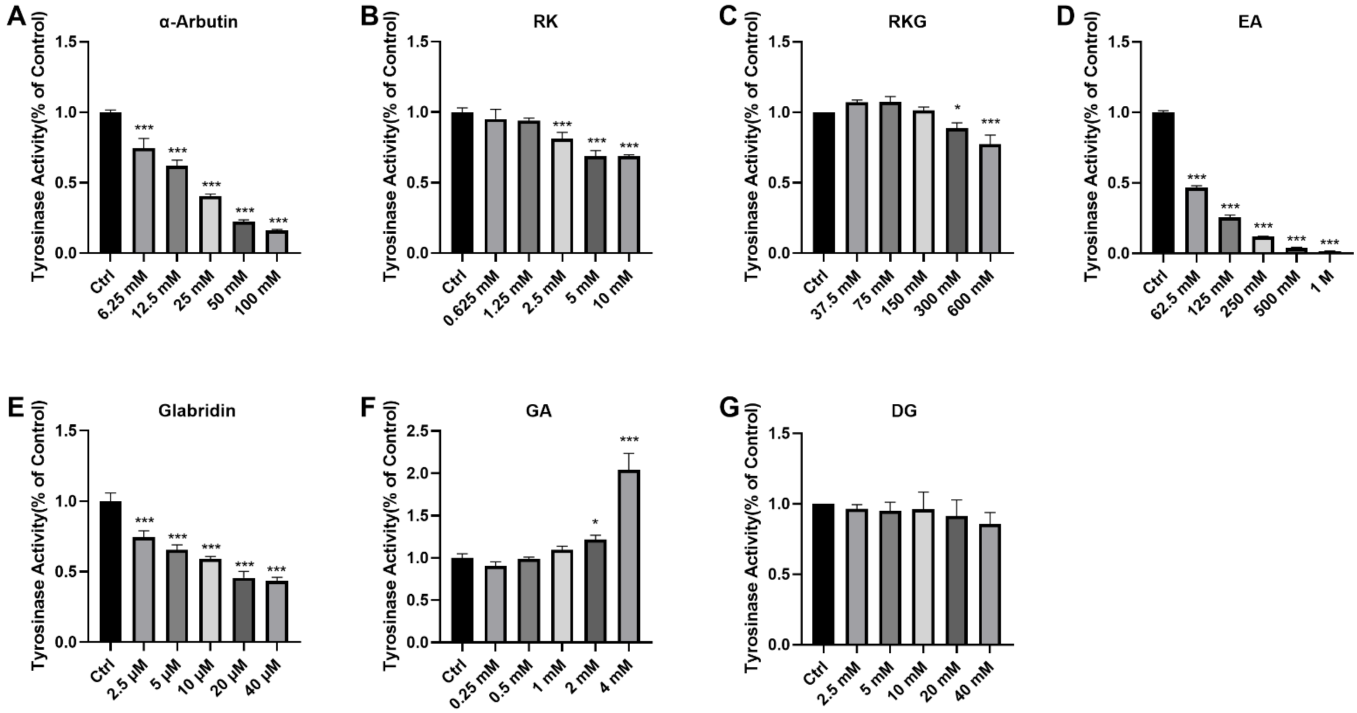

Figure 2. (A-G) The effects of anti-hyperpigmentation compounds on mushroom tyrosinase assay. (A) Tyrosinase activity of α-arbutin with the concentration of (0-100 mM). (B) Tyrosinase activity of RK with the concentration of (0-10 mM). (C) Tyrosinase activity of RKG with the concentration of (0-600 mM). (D) Tyrosinase activity of EA with the concentration of (0-1 M). (E) Tyrosinase activity of Glabridin with the concentration of (0-40 μM). (F) Tyrosinase activity of GA with the concentration of (0-4 mM). (G) Tyrosinase activity of DG with the concentration of (0-40 mM). Results are shown as mean ± standard error of the mean * $p<0.05$, ** $p<0.01$, *** $p<0.001$.

B16-F10 Mouse Melanoma Cells Model

Tyrosinase Activity of B16-F10 Cells Model

B16-F10 cells can be used to determine whether anti-hyperpigmentation compounds can inhibit tyrosinase activity and melanin production. Tyrosinase activity of B16-F10 cells is an important index for evaluating anti-hyperpigmentation capability. The experimental concentration was determined using the results of the CCK8 assay, as shown in Figure 3. The inhibition of tyrosinase activity in B16-F10 mouse melanoma cells was shown in Figure 4. Four of these seven compounds have significant difference compare with blank group. The maximum inhibitory concentrations of these compounds were 64.52 % (80 mM) for α-arbutin, 41.01 % (40 μM) for GLA, 47.88 %(10 μM) for GA, and 11.35 % (1 mM) for DG. EA, RK and RKG had no inhibitory effect on the tyrosinase activity.

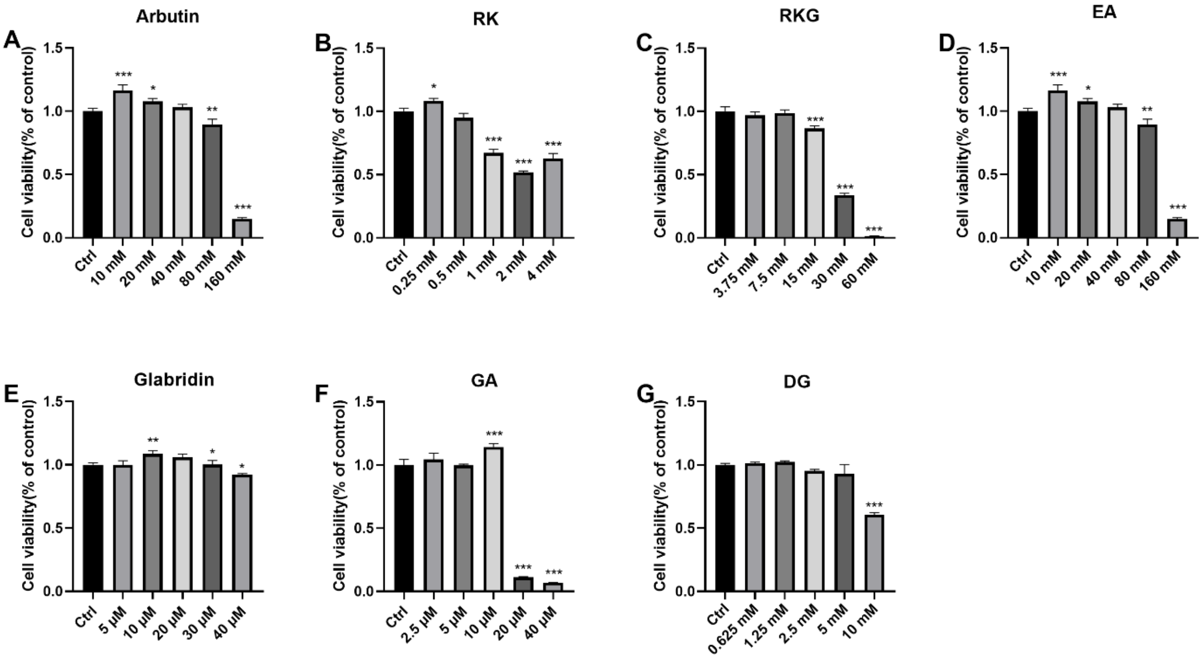

Figure.3. (A-G) The cellular viability of anti-hyperpigmentation ingredients on B16-F10 melanoma cells were examined after 48 h of treatment. (A). Cellular viability of α-Arbutin with the concentration of (0-160 mM). (B). Cellular viability of RK with the concentration of (0-4 mM). (C). Cellular viability of RKG with the concentration of (0-60 mM). (D). Cellular viability of EA with the concentration of (0-160 M). (E) . Cellular viability of Glabridin with the concentration of (0-40 μM). (F) . Cellular viability of GA with the concentration of (0-40 μM). (G). Cellular viability of DG with the concentration of (0-10 mM). Results are shown as mean ± standard error of the mean * p<0.05, ** p<0.01, *** p<0.001.

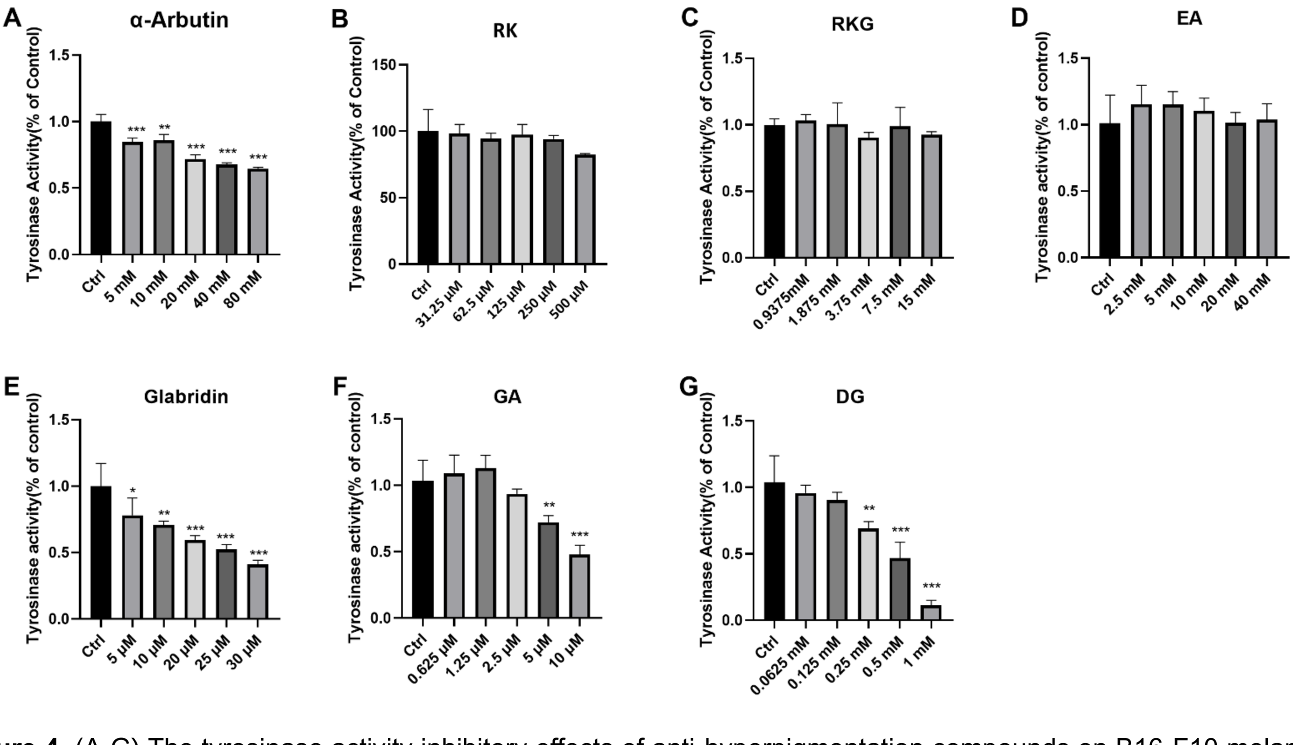

Figure 4. (A-G) The tyrosinase activity inhibitory effects of anti-hyperpigmentation compounds on B16-F10 melanoma cells were examined after 48 h of treatment. (A) Tyrosinase activity of α-arbutin with the concentration of (0-80 mM). (B) Tyrosinase activity of RK with the concentration of (0-500 μM). (C) Tyrosinase activity of RKG with the concentration of (0-15 mM). (D) Tyrosinase activity of EA with the concentration of (0-40 mM). (E) Tyrosinase activity of Glabridin with the concentration of (0-30 μM). (F) Tyrosinase activity of GA with the concentration of (0-10 μM). (G) Tyrosinase activity of DG with the concentration of (0-1 mM). Results are shown as mean ± standard error of the mean * p<0.05, ** p<0.01, *** p<0.001.

Melanin Content of B16-F10 Cells Model

Melanin is the final product of the complete melanin biosynthesis pathway. Anti-hyperpigmentation ingredient is described with respect to melanin formation. As shown in Figure 5, there were six compounds inhibiting melanin content; only GA had no melanin inhibitory effect. They reduced melanin synthesis in a dose-dependent manner without significant toxicity. The maximum inhibitory concentrations of five of the seven compounds were as follows: 47.35 % (80 mM) for α-arbutin, 35.19 % (500 μM) for RK, 55.41 % (15 mM) for RKG, 4.31 % (15 mM) for EA, 13.97 % (40 μM) for GLA, and 8.91 % (1 mM) for DG. GA had no inhibitory effect on melanin production in B16-F10 mouse melanoma cells.

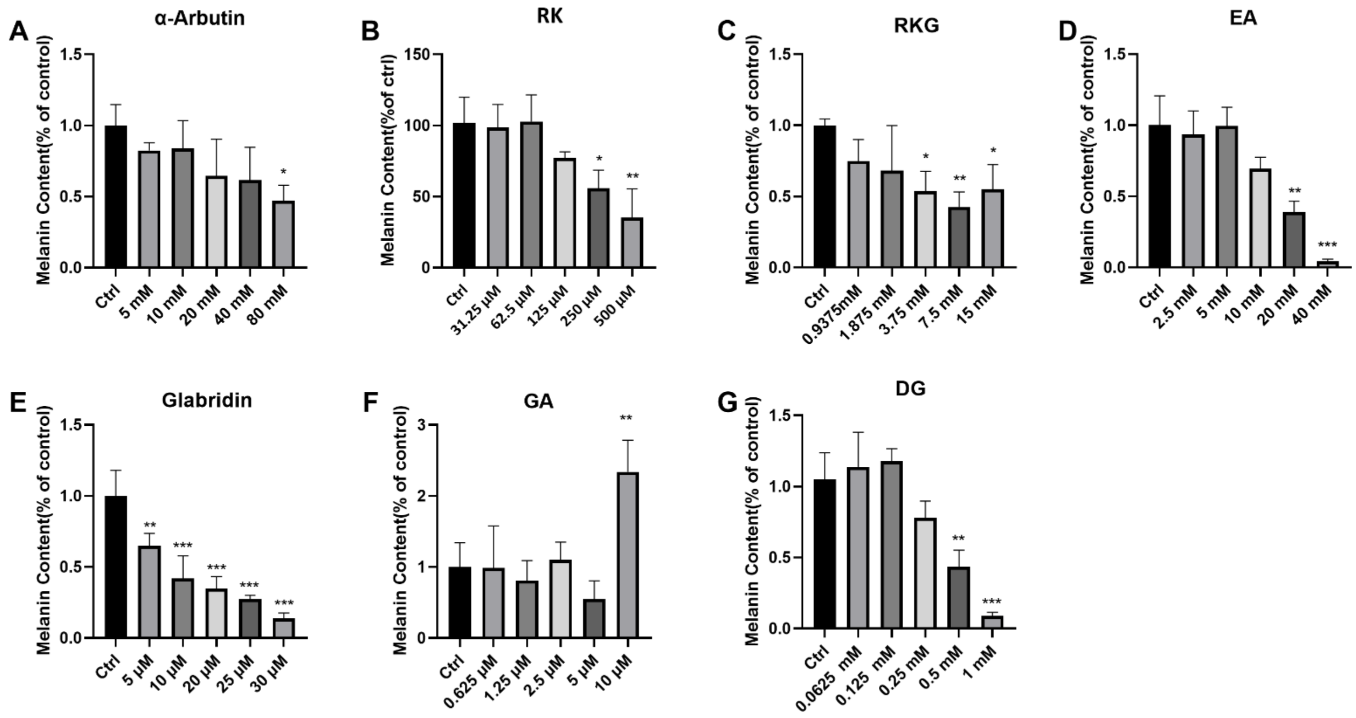

Figure 5. (A-G) The melanin inhibition effects of anti-hyperpigmentation compounds on B16-F10 melanoma cells were examined after 48 h of treatment. (A) Melanin contents of α-arbutin with the concentration of (0-80mM). (B) Melanin contents of RK with the concentration of (0-500 μM). (C) Melanin contents of RKG with the concentration of (0-15 mM). (D) Melanin contents of EA with the concentration of (0-40mM). (E) Melanin contents of Glabridin with the concentration of (0-30 μM). (F) Melanin contents of GA with the concentration of (0-10 μM). (G) Melanin contents of DG with the concentration of (0-1 mM). Results are shown as mean ± standard error of the mean * $p<0.05$, ** $p<0.01$, *** $p<0.001$.

Zebrafish Model

Tyrosinase Activity of Zebrafish Model

The zebrafish model was used as an in vivo system to evaluate the inhibition of melanogenesis. We evaluated the whitening effect of anti-hyperpigmentation compounds on zebrafish tyrosinase activity and melanin formation in zebrafish embryos. The experimental concentrations were determined from the results of the cytotoxicity assay. As shown in Figure 6, the five compounds inhibited tyrosinase activity in zebrafish. The maximum inhibitory concentrations of these five compounds were 48.52 % (100 mM) for α-arbutin, 53.32 % (80 μM) for RK, 81.07 % (1 mM) for RKG, 67.00 % (150 mM) for EA, and 67.39 % (30 μM) for GA. DG and GLA did not inhibit the tyrosinase activity.

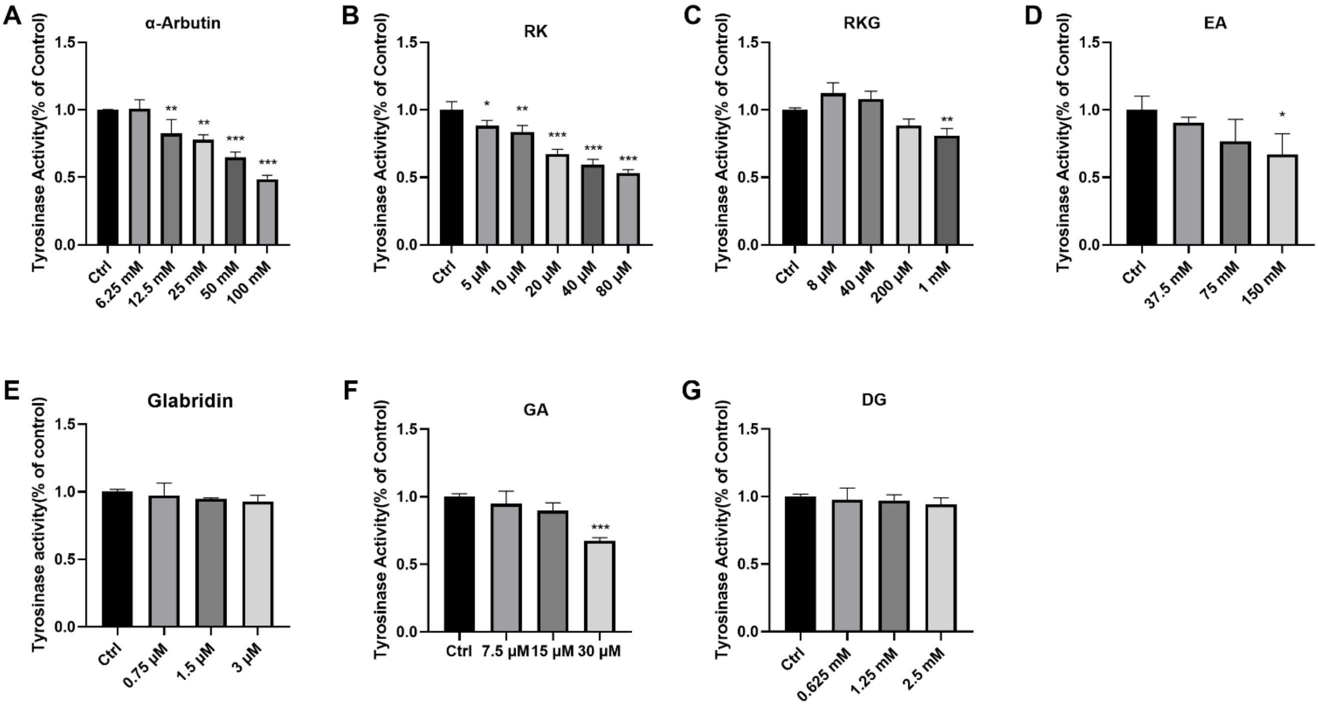

Figure 6. (A-G) The tyrosinase activity inhibition effects of anti-hyperpigmentation compounds on zebrafish were examined after 48 h of treatment. (A) Tyrosinase activity of α-arbutin with the concentration of (0-100 mM). (B) Tyrosinase activity of RK with the concentration of (0-80 μM). (C) Tyrosinase activity of RKG with the concentration of (0-1 mM). (D) Tyrosinase activity of EA with the concentration of (0-150 mM). (E) Tyrosinase activity of Glabridin with the concentration of (0-3 μM). (F) Tyrosinase activity of GA with the concentration of (0-30 μM). (G) Tyrosinase activity of DG with the concentration of (0-2.5 mM). Results are shown as mean ± standard error of the mean * p<0.05, ** p<0.01, *** p<0.001.

Melanin Content of Zebrafish Model

The melanin content of zebrafish embryos was visually observed in the images captured by the microscope. By analyzing the images, we were able to perform further quantitative analyses. We developed a Python program, which can directly reduce the amount of work and time required. We verified by comparison that the result of the program is consistent with the result of using ImageJ software, as shown in Figure 7. As shown in Figures 8 and 9 in the zebrafish model, α-arbutin, RK, RKG, and GA significantly reduced the melanin content on zebrafish's surface. As shown in Figure 8, the maximum inhibitory concentrations of these three compounds were 33.47 % (100 mM) for α-arbutin, 16.71 % (80 μM) for RK, 8.62 % (1 mM) for RKG, 71.28 % (30 μM) for GA. EA, DG and GLA had no inhibitory effect on melanin production in zebrafish.

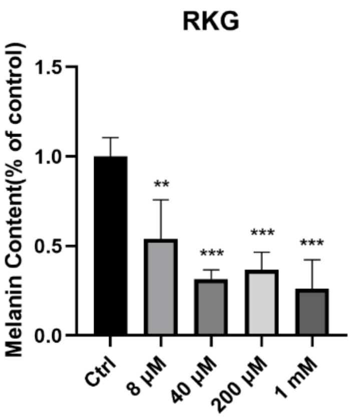

Figure 7. Results are shown as mean ± standard error of the mean * p<0.05, ** p<0.01, *** p<0.001.

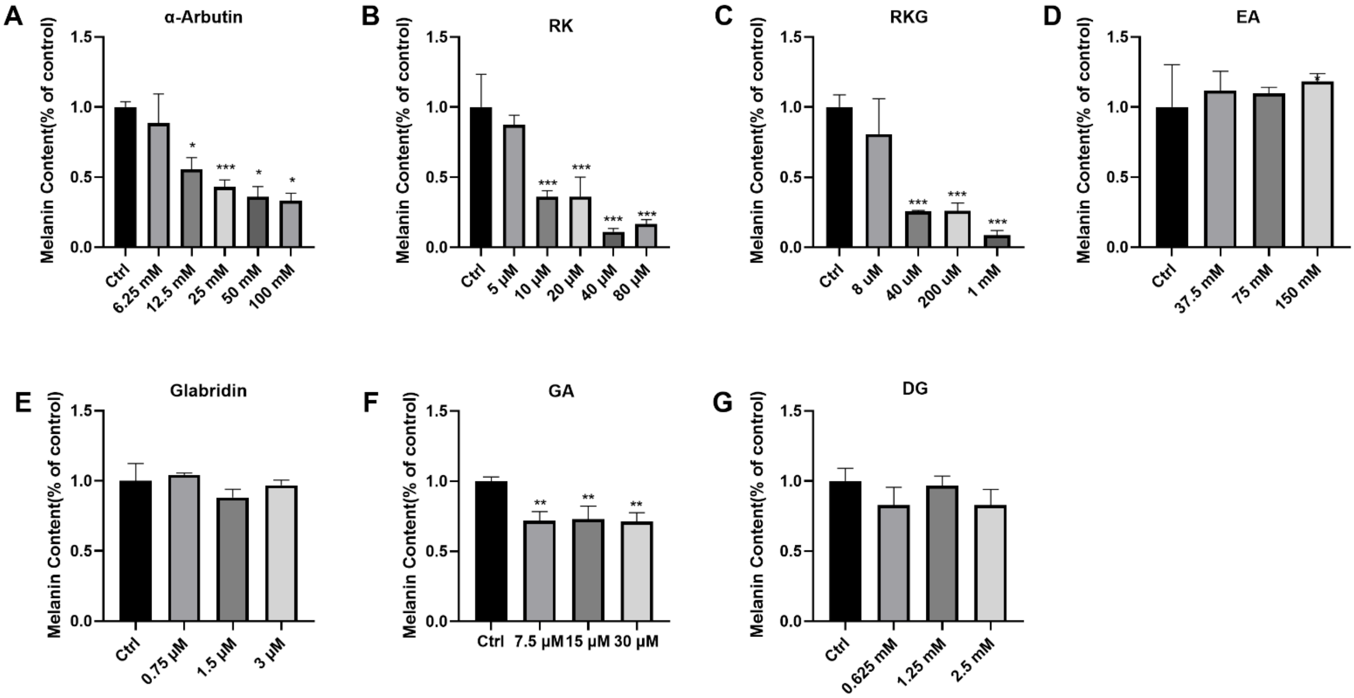

Figure 8. (A-G) The melanin inhibition effects of anti-hyperpigmentation compounds on zebrafish were examined after 48 h of treatment. (A) Melanin contents of α-arbutin with the concentration of (0-100 mM). (B) Melanin contents of RK with the concentration of (0-80 μM). (C) Melanin contents of RKG with the concentration of (0-1 mM). (D) Melanin contents of EA with the concentration of (0-150 mM). (E) Melanin contents of Glabridin with the concentration of (0-3 μM). (F) Melanin contents of GA with the concentration of (0-30 μM). (G) Melanin contents of DG with the concentration of (0-2.5 mM). Results are shown as mean ± standard error of the mean * p<0.05, ** p<0.01, *** p<0.001.

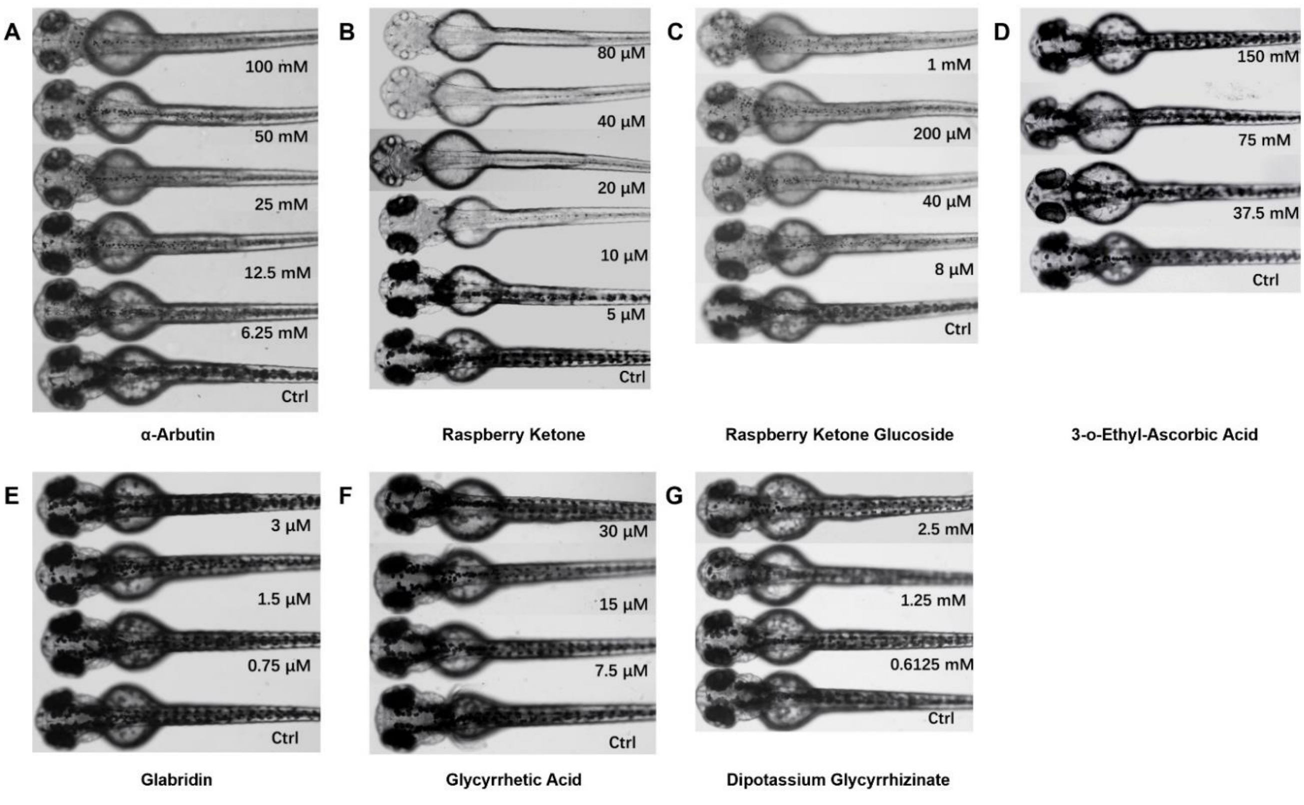

Figure 9. (A-G) The melanin contents of anti-hyperpigmentation compounds on zebrafish were examined after 48 h of treatment. (A) Tyrosinase activity of α-arbutin with the concentration of (0-100 mM). (B) Tyrosinase activity of RK with the concentration of (0-80 μM). (C) Tyrosinase activity of RKG with the concentration of (0-1 mM). (D) Tyrosinase activity of EA with the concentration of (0-150 mM). (E) Tyrosinase activity of Glabridin with the concentration of (0-3 μM). (F) Tyrosinase activity of GA with the concentration of (0-30 μM). (G) Tyrosinase activity of DG with the concentration of (0-2.5 mM).

DISCUSSION

The MTA, B16-F10 cell model and zebrafish were used to evaluate the whitening efficacy of the seven compounds in our study. The results are presented in Table 1. In summary, most of the results in this manuscript are consistent with previous publications, while some are conflicting. Our data verified previous conclusions and raised new questions for future investigations.

Table 1. Results of three models.

Bioactive Compounds	Description	ICmt	ICbm	ICbt	ICzm	ICzt
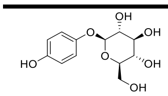 α-Arbutin	Formula: $C_{12}H_{16}O_7$ MW:272.25 Origin: Synthetic	16.21 % 100 mM	47.35% 80 mM	64.52% 80 mM	33.47% 100 mM	48.52% 100 mM
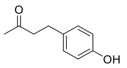 Raspberry Ketone	Formula: $C_{10}H_{12}O_2$ MW:164.2 Origin: Raspberry	68.77 % 10 mM	35.19 % 500 μM	82.34 % 500 μM	16.71% 80 μM	53.32% 80 μM
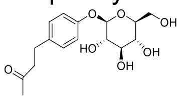 Raspberry Ketone Glucoside	Formula: $C_{16}H_{22}O_7$ MW: 326.34 Origin: Rhizoma Rhei	77.21 % 600 mM	55.14 % 15 mM	92.40 % 15 mM	8.62% 1 mM	81.07% 1 mM
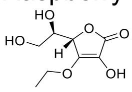 3-o-Ethyl-Ascorbic	Formula: $C_8H_{12}O_6$ MW: 204.18 Origin: Synthetic	1.48 % 1 M	4.31 % 15 mM	103.84% 15 mM	118.2% 150 mM	67.00% 150 mM
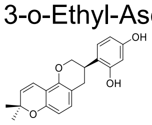 Glabridin	Formula: $C_{20}H_{20}O_4$ MW:324.37 Origin: Licorice	43.55 % 40 μM	13.97 % 30 μM	41.01 % 30 μM	96.86% 3 μM	92.76% 3 μM
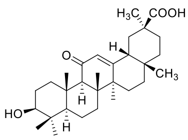 Glycyrrhetic Acid	Formula $C_{30}H_{46}O_4$: MW: 470.69 Origin: Licorice	204.18 % 4 mM	233.88 % 10 μM	47.88 % 10 μM	71.28% 30 μM	67.39% 30 μM
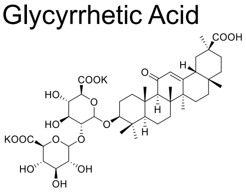 Dipotassium Glycyrrhizinate	Formula: $C_{42}H_{60}K_2O_{16}$ MW: 899.1128 Origin: Licorice	85.87 % 40 mM	8.91 % 1 mM	11.35 % 1 mM	82.93 % 2.5 mM	94.42 % 2.5 mM

MW = molecular weight (g/mol); ICmt=mushroom tyrosinase activity; ICbm = B16-F10 melanoma cells melanin content level; ICbt = B16-F10 melanoma cells tyrosinase activity; ICzm = zebrafish melanin content level; ICzt = zebrafish tyrosinase activity. ICmt, ICbm, ICbt, ICzm, and ICzt in percentage (%)compared to untreated control.

α-Arbutin, which has been reported to inhibit melanin production in B16-F10 cells and inhibit tyrosinase activity of MTA, has been widely used in the cosmetics industry. Our results on α-arbutin are broadly consistent with previous reports [16, 17] (Figures 2A, 4A, 5A). Besides, we provide evidence that α-arbutin inhibits melanin and tyrosinase activity in a zebrafish model for the first time (Figures 6A, 8A, 9A).

Both RK and RKG are the main "aromatic compounds" derived from raspberries and are used as fragrances in food processing and cosmetics[18]. Previous research has shown that RK has inhibitory effects on mushroom tyrosinase, B16-F10 cells, and zebrafish[19, 20]. Our results are consistent with those of previous studies (Figures 2B, 4B, 5B, 6B, 8B, 9B). RK is a glycosyl of RKG, but its biological activity is different. RKG was found to inhibit melanin production in B16-F10 cells [21]. Similar to RK, RKG decreased melanin content (Figures 6C, 8C, 9C). However, RKG did not affect tyrosinase activity, suggesting that RK and RKG may have different melanin inhibition mechanisms (Figures 2C, 4C, 5C).

Vitamin C is used as a traditional whitening ingredient, but it has poor photostability[22]. EA is a highly-stable derivative of Vitamin C. Only the inhibition of mushroom tyrosinase by EA has been reported (Figure 2D) [23]. Our results showed that EA decreased melanin content in B16-F10 cells, but had no effect on tyrosinase activity (Figure 4D,5D). In the zebrafish model, EA neither inhibit melanin production nor tyrosinase activity (Figures 6D, 8D, 9D). Therefore, the anti-pigmentation activity of EA in vivo requires further investigation. We speculated that although EA has an inhibitory effect on tyrosinase activity in vitro, the anti-pigmentation activity of EA may not be directly related to tyrosinase independent pathway in B16-F10 cells. And we also speculated that EA is difficult to penetrate the epidermis of zebrafish embryos because of its high-water solubility. Therefore, EA has no anti-pigmentation activity in zebrafish model. This assumption needs to be further investigation.

Glycyrrhiza glabra Linn extract is mentioned in the list of anti-hyperpigmentation compounds, among which the representative compounds are GA, DG, and GLA[24, 25]. GA has been reported to be a potential anticancer agent [24]. We found that GA promoted mushroom tyrosinase activity; however, it slightly inhibited melanin production and tyrosinase activity in zebrafish (Figures 2F, 6F, 8F, 9F). GA promoted melanin content and inhibited tyrosinase activity in B16-F10 cells (Figures 4F, 5F). The specific mechanism needs to be studied further. DG has been shown in previous studies to reduce inflammation, but no study has reported its whitening effect[26]. The results showed that DG inhibited melanin production and tyrosinase activity in B16-F10 cells and showed no significant inhibition in the zebrafish model for the first time (Figures 2G, 4G, 5G, 6G,8G, 9G). We verified that GLA could inhibit tyrosinase activity in MTA (Figure 2E), melanin production in the B16-F10 model, and not decrease melanin production in the zebrafish model, which is consistent with a previous study[9, 10] (Figures 4E, 5E, 6E, 8E, 9E). The safe concentration of GLA in the zebrafish model was lower than that in the B16-F10 cell model. Therefore, we hypothesized that GLA could not inhibit melanin production at tolerance concentrations in the zebrafish model.

In summary, we evaluated seven anti-hyperpigmentation compounds listed, via the three most widely used screening methods. Most of the results are consistent with previous studies, although not all of them are effective.

Tyrosinase is the rate-limiting enzyme in melanogenesis. Therefore, mushroom tyrosinase activity assay is widely used to evaluate the potential whitening effect of whitening compounds ex vivo. However, we found that the results of the mushroom tyrosinase assay were different from those of the other two models, as shown by the results of RKG and DG (Figures 2C, 2G). Therefore, MTA alone can lead to false-negative results in anti-hyperpigmentation ingredient screening.

B16-F10 cells have also been widely used in pigmentation studies. In our study, B16-F10 cells showed the highest rate of positive results. However, melanin production in the B16-F10 cell model was unstable, leading to poor repeatability of results. Based on the ATCC guidelines, the recommended medium for B16-F10 was RPMI 1640. We found that B16-F10 cells cultured in RPMI 1640 medium had a poor ability to produce melanin, but had better proliferation ability. B16-F10 cells cultured in DMEM medium had a good ability to produce melanin, but poor in proliferation. Thus, we used RPMI 1640 medium for cell culture only, and changed into DMEM medium for reagent effective experiment.

Zebrafish have a long history of pigmentation research and high-throughput screening. Compared with B16-F10 cells, the zebrafish model can simulate different stages of melanin maturation. In our study, zebrafish showed the most negligible positive results among the three models. We speculate that this might be due to zebrafish being an in vivo model. Zebrafish can maintain homeostasis, which may affect the absorption or metabolism of compounds. Previous studies have speculated that different molecular weights of compounds may influence absorption[7]. The lighter molecular weight makes it easier to penetrate the zebrafish skin. This may be since the least number of compounds showed positive results.

In previous studies, most of the seven anti-hyperpigmentation compounds have been shown to have practical applications in human skin experiments. α-arbutin has been studied and applied to a 3D human skin model, and it has been shown that α-arbutin can effectively reduce melanin content [27]. The results are the same as the results of the three models (Figures 2A, 4A, 5A, 6A, 8A, 9A). GLA is used extensively in the cosmetic industry as a skin-whitening agent [28, 29]. EA has been studied to reduce melanin in human skin preparations containing this compound[30]. RKG was used in cosmetic product formulations, and human experiments proved that the product could reduce melanin-induced whitening of the skin [31]. GA has been studied in the human body in the form of nano-formulations[32], and DG preparation was used in the human skin transdermal absorption model [33]. There are no relevant studies on RK in human skin models.

Thus, most of these compounds have been tested in humans and 3D human skin. The results agreed well with the experimental results, whereas screening bias existed within the results. GLA and EA showed negative results in the zebrafish model (Figures 8D,8E); however, cosmetics containing GLA or EA have shown that both can reduce melanin content in human skin[28-30]. Zebrafish models may not be suitable for evaluating GLA, EA, and their derivatives, and false-negative results may occur. We hypothesized that GLA and EA could not inhibit melanin production at tolerance concentrations in the zebrafish model. Further research is needed to understand the mechanisms underlying their whitening effect.

In conclusion, mushroom tyrosinase analysis is the most convenient assay among the three models but has poor reliability. The B16-F10 mouse melanoma cell model was the most sensitive but had poor stability. The B16-F10 model requires the experimenter to have higher practical skills. The zebrafish model has better repeatability than other models; however, in the in vivo model, most of the compounds were difficult to screen. When a lab has certain required conditions, these models should be integrated to evaluate whitening effects. The experimental results are valuable for the practical application of these compounds.

Funding: This work was supported by The National Science Foundation of China [grant number :81802123].
Conflicts of Interest: The authors declare no conflict of interest

REFERENCES

1. Pillaiyar T, Manickam M, Jung SH. Recent development of signaling pathways inhibitors of melanogenesis. Cell Signal. 2017;40:99-115. doi: 10.1016/j.cellsig.2017.09.004, PMID 28911859.
2. Liu JJ, Fisher DE. Lighting a path to pigmentation: mechanisms of MITF induction by UV. Pigment Cell Melanoma Res. 2010;23(6):741-5. doi: 10.1111/j.1755-148X.2010.00775.x, PMID 20973930.
3. Ishak N, Lajis AFB, Mohamad R, Ariff AB, Mohamed MS, Halim M, Wasoh H. Kinetics and optimization of lipophilic kojic acid derivative synthesis in polar aprotic solvent using lipozyme RMIM and its rheological study. Molecules. 2018;23(2):501. doi: 10.3390/molecules23020501, PMID 29495254.
4. Pillaiyar T, Manickam M, Namasivayam V. Skin whitening agents: medicinal chemistry perspective of tyrosinase inhibitors. J Enzyme Inhib Med Chem. 2017;32(1):403-25. doi: 10.1080/14756366.2016.1256882, PMID 28097901.
5. Colombo S, Berlin I, Delmas V, Larue L. Chapter 2: classical and nonclassical melanocytes in vertebrates. In: Borovanský Prof J, Riley Prof PA, editors Melanins and melanosomes: biosynthesis, biogenesis, physiological, and pathological functions; 2011. p. 21-61.
6. Nagendra Prasad K, Yang B, Yang S, Chen Y, Zhao M, Ashraf M, et al. Identification of phenolic compounds and appraisal of antioxidant and antityrosinase activities from litchi (Litchi sinensis Sonn.) seeds. Food Chem. 2009;116(1):1-7. doi: 10.1016/j.foodchem.2009.01.079.
7. Lajis AFB. A zebrafish embryo as an animal model for the treatment of hyperpigmentation in cosmetic dermatology medicine. Medicina (Kaunas). 2018;54(3):35. doi: 10.3390/medicina54030035, PMID 30344266.
8. Langheinrich U. Zebrafish: A new model on the pharmaceutical catwalk. BioEssays. 2003;25(9):904-12. doi: 10.1002/bies.10326, PMID 12938180.
9. Yokota T, Nishio H, Kubota Y, Mizoguchi M. The inhibitory effect of glabridin from licorice extracts on melanogenesis and inflammation. Pigment Cell Res. 1998;11(6):355-61. doi: 10.1111/j.1600-0749.1998.tb00494.x, PMID 9870547.
10. Chen J, Yu X, Huang Y. Inhibitory mechanisms of glabridin on tyrosinase. Spectrochim Acta A Mol Biomol Spectrosc. 2016;168:111-7. doi: 10.1016/j.saa.2016.06.008, PMID 27288962.
11. Wang C, Liu BJ, He C. Review and management of whitening cosmetics in China and in the world. Beijing Daily. 2015 [Suppl]*)* Special Issue on whitening:42-7.
12. General administration of quality supervision, I.a.Q.o.t.P.s.R.o.C, Determination of 10 whitening in cosmetics by high-performance liquid chromatography. In: (*GBT 35954-2018*). Standards press of China. Beijing 2018.
13. Mohd Sakeh N, Md Razip NN, Mohd Ma'in FI, Abdul Bahari MN, Latif N, Akhtar MN, et al. Melanogenic inhibition and toxicity assessment of flavokawain A and B on B16/F10 melanoma cells and zebrafish (*Danio rerio*). Molecules;25(15):3403. doi: 10.3390/molecules25153403.
14. Yokozawa T, Kim YJ. Piceatannol inhibits melanogenesis by its antioxidative actions. Biol Pharm Bull. 2007;30(11):2007-11. doi: 10.1248/bpb.30.2007, PMID 17978467.
15. Jayachandra R, Zhao H, Cheng Z, Luo L, Sun T, Tan W. Synthesis of isosteviol analogues as potential protective agents against doxorubicin-induced cardiomyopathy in zebrafish embryos. Bioorg Med Chem Lett. 2019;29(14):1705-9. doi: 10.1016/j.bmcl.2019.05.033, PMID 31129053.
16. Qin L, Wu Y, Liu Y, Chen Y, Zhang P. Dual effects of alpha-arbutin on monophenolase and diphenolase activities of mushroom tyrosinase. PLoS One. 2014;9(10):e109398. doi: 10.1371/journal.pone.0109398, PMID 25303458.
17. Song NY, Cho JG, Im D, Lee DY, Wu Q, Seo WD, et al. Triterpenoids from *Fragaria ananassa* calyx and their inhibitory effects on melanogenesis in B16-F10 mouse melanoma cells. Nat Prod Res. 2013;27(23):2219-23. doi: 10.1080/14786419.2013.805330, PMID 23772756.
18. Kim BS. Microbial production of natural raspberry ketone. Biotechnol Bioeng. 2010;43.
19. Ito S, Hinoshita M, Suzuki E, Ojika M, Wakamatsu K. Tyrosinase-catalyzed oxidation of the leukoderma-inducing agent raspberry ketone produces (E)-4-(3-oxo-1-butenyl)-1,2-benzoquinone: implications for melanocyte toxicity. Chem Res Toxicol. 2017;30(3):859-68. doi: 10.1021/acs.chemrestox.7b00006, PMID 28219012.
20. Lin CHV, Ding HY, Kuo SY, Chin LW, Wu JY, Chang TS. Evaluation of in vitro and in vivo depigmenting activity of raspberry ketone from Rheum officinale. Int J Mol Sci. 2011;12(8):4819-35. doi: 10.3390/ijms12084819, PMID 21954327.
21. Yokota T, Ikemoto T, Sasaki M, Horikoshi T. Lasting effect of raspberry ketone glucoside on whitening. J Soc Cosmet Chem Japan. 2001;35(2):120-6. doi: 10.5107/sccj.35.2_120.
22. Colven RM, Pinnell SR. Topical vitamin C in aging. Clin Dermatol. 1996;14(2):227-34. doi: 10.1016/0738-081x(95)00158-c, PMID 8860861.

23. Iliopoulos F, Sil BC, Moore DJ, Lucas RA, Lane ME. 3-O-ethyl-l-ascorbic acid: characterisation and investigation of single solvent systems for delivery to the skin. Int J Pharm X. 2019;1. doi: 10.1016/j.ijpx.2019.100025.
24. Li J, Tang F, Li R, Chen Z, Lee SY, Fu C, et al. Dietary compound glycyrrhetinic acid suppresses tumor angiogenesis and growth by modulating antiangiogenic and proapoptotic pathways *in vitro* and *in vivo*;77. doi: 10.8268(2020).
25. Shim JY, Yim SB, Chung JH, Hong KS. Antiplaque and antigingivitis effects of a mouthrinse containing cetylpyridinium chloride, triclosan and dipotassium glycyrrhizinate. J Periodontal Implant Sci. 2012;42(2):33-8. doi: 10.5051/jpis.2012.42.2.33, PMID 22586520.
26. Lee SH, Bae IH, Choi H, Choi HW, Oh S, Marinho PA, et al. Ameliorating effect of dipotassium glycyrrhizinate on an IL-4- and IL-13-induced atopic dermatitis-like skin-equivalent model. Arch Dermatol Res. 2019;311(2):131-40. doi: 10.1007/s00403-018-1883-z, PMID 30506356.
27. Sugimoto K, Nishimura T, Nomura K, Sugimoto K, Kuriki T. Inhibitory effects of alpha-arbutin on melanin synthesis in cultured human melanoma cells and a three-dimensional human skin model. Biol Pharm Bull. 2004;27(4):510-4. doi: 10.1248/bpb.27.510, PMID 15056856.
28. Wang X, Zhou L, Chai B. The application, extraction and separation and preparation methods for glabridin. Fine Chem Intermed. 2020;50(06):10-5. (in Chinese).
29. Simmler C, Pauli GF, Chen SN. Phytochemistry and biological properties of glabridin. Fitoterapia. 2013;90:160-84. doi: 10.1016/j.fitote.2013.07.003, PMID 23850540.
30. Nan W. Study on the whitening efficacy of ascorbic acid ethyl ether. Beijing Daily. 2016;6:40-5. (in Chinese).
31. Anliang LI, Yang S, Guo X. Research and Development on cosmetic actives derived from raspberry ketone glucoside. Flavour Fragr Cosmet. 2014.
32. Puglia C, Rizza L, Drechsler M, Bonina F. Nanoemulsions as vehicles for topical administration of glycyrrhetic acid: characterization and in vitro and in vivo evaluation. Drug Deliv. 2010;17(3):123-9. doi: 10.3109/10717540903581679, PMID 20136625.
33. Trotta M, Peira E, Debernardi F, Gallarate M. Elastic liposomes for skin delivery of dipotassium glycyrrhizinate. Int J Pharm. 2002;241(2):319-27. doi: 10.1016/s0378-5173(02)00266-1, PMID 12100859.